Liquid-Erosion Failures

Frederick G. Hammitt, Department of Mechanical Engineering and Applied Mechanics, University of Michigan
Frank J. Heymann, Westinghouse Electric Corporation

EROSION of a solid surface can take place in a liquid medium even without the presence of solid abrasive particles in that medium. Cavitation, one mechanism of liquid erosion, involves the formation and subsequent collapse of bubbles within the liquid. The process by which material is removed from a surface is called cavitation erosion, and the resulting damage is termed cavitation damage. The collision at high speed of liquid droplets with a solid surface results in a form of liquid erosion called liquid-impingement erosion.

Cavitation damage has been observed on ship propellers and hydrofoils; on dams, spillways, gates, tunnels, and other hydraulic structures; and in hydraulic pumps and turbines. High-speed flow of liquid in these devices causes local hydrodynamic pressures to vary widely and rapidly. In mechanical devices, severe restrictions in fluid passages have produced cavitation damage downstream of orifices and in valves, seals, bearings, heat-exchanger tubes, and venturis. Cavitation erosion has also damaged water-cooled diesel-engine cylinder liners.

Liquid-impingement erosion has been observed on many components exposed to high-velocity steam containing moisture droplets, such as blades in the low-pressure end of large steam turbines. Rain erosion, one form of liquid-impingement erosion, frequently damages the aerodynamic surfaces of aircraft and missiles when they fly through rainstorms at high subsonic or supersonic speeds. Liquid-impingement and cavitation erosion are of concern in nuclear-power systems, which operate at lower steam quality than conventional steam systems, and in systems using liquid metals as the working fluid, where the corrosiveness of the liquid metal can promote rapid erosion of components.

Liquid erosion involves the progressive removal of material from a surface by repeated impulse loading at microscopically small areas. Liquid dynamics is of major importance in producing damage, although corrosion also plays a role in the damage process, at least with certain fluid-material combinations. The process of liquid erosion is not as well understood as most other failure processes. It is difficult to define the hydrodynamic conditions that produce erosion and the metallurgical processes by which particles are detached from the surface. Evidently, both cavitation and liquid impingement exert similar hydrodynamic forces on a solid surface. In any event, the appearance of damaged surfaces and the relative resistance of materials to damage are similar for both liquid-impingement and cavitation erosion.

Cavitation

When the local pressure in a liquid is reduced without a change in temperature, a condition may eventually be reached where gas-filled bubbles (or cavities) nucleate and grow within the body of liquid. The gas in the bubbles may be vapor or molecules of a substance that was formerly dissolved in the liquid. If a bubble is formed by vaporization, bubble growth will occur rapidly, but if gas dissolution is required for bubble formation, growth will occur more slowly. Growth of gas-filled bubbles (as opposed to vapor-filled bubbles) depends on the diffusion of dissolved gas to the cavity or on the rate of gas expansion due to pressure reduction. If cavities formed in a low-pressure region pass into a region of higher pressure, their growth will be reversed, and they will collapse and disappear as the vapor condenses or the gas is redissolved in the liquid. A vapor-filled cavity will implode, collapsing very rapidly (perhaps within a few milliseconds); a gas-filled cavity will collapse more slowly—both being the exact or nearly exact reverse of the bubble-growth process (the liquid dynamics of bubble growth and collapse are covered in Ref 1 and 2).

The collapse of cavities (bubbles) produces the damage to materials. The exact mechanism by which cavity collapse transmits severe localized forces to a surface is not fully understood. However, it most likely involves either waves produced by the collapse and immediate reformation of a cavity, a process known as rebound (Fig. 1), or impingement of a microjet of liquid through the collapsing cavity onto the surface being damaged due to nonsymmetrical cavity collapse (Fig. 2). Both rebound and nonsymmetrical collapse with formation of microjet have been observed experimentally and partly computed analytically (Ref 1, 2).

Collapse pressures were first estimated by Lord Rayleigh in 1917 and have since been estimated by many others using modifications of Rayleigh's theory. Rayleigh found that, for an empty cavity collapsing with spherical symmetry in an incompressible inviscid fluid, the velocity of the collapsing cavity wall and the pressure at the instant of complete collapse were infinitely large. Later analyses, many of which were based on the assumption of adiabatic compression of gas in a collapsing cavity in a compressible fluid, predicted collapse pressures in the range of 30 to 223 MPa (300 to 2200 atm). Although more recent analyses predict wall velocities approaching infinity for a spherical empty cavity at the instant of complete collapse, the presence of gas within the cavity results in wall velocities that rise to a very high value immediately before complete collapse, then fall rapidly to zero at the instant of collapse. Later computer analyses (Ref 2) show more

Fig. 1 The mechanics of cavity growth, collapse, and rebound

(a) Schematic representation of successive stages of growth, collapse, and rebound of a single traveling cavity. (b) Graph of cavity diameter as a function of time for the cavity in (a). Source: Ref 1

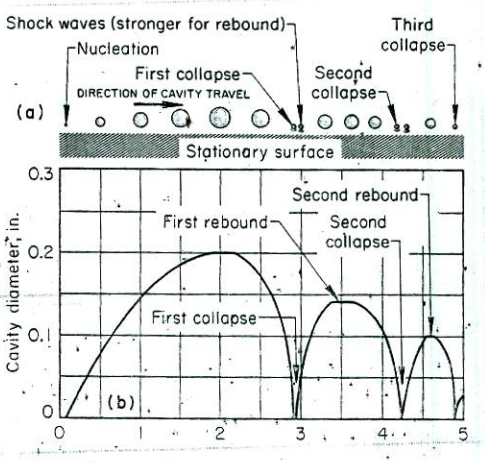

successive stages of nonsymmetrical cavity collapse with microjet impingement against a metallic surface

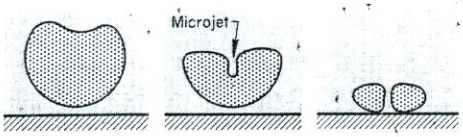

realistic results for symmetrical and nonsymmetrical collapses with real fluid parameters.

Actual collapses near a surface do not preserve spherical symmetry very far into the collapse; thus, the Rayleigh model is largely voided. Actual collapses form microjets of liquid (Fig. 2), which probably attain velocities from 100 to 500 m/s (330 to 1640 ft/s). Thus, the actual damaging process may be quite similar to that of liquid impingement, except the jet is much smaller (a few microns in diameter).

One aspect of the collapse of a gas-filled cavity is important: in order to retard collapse significantly and thereby reduce the amount of resulting damage, the gas must be capable of storing much of the thermodynamic work involved in collapsing the cavity. Cavitation usually occurs in a liquid of low vapor pressure and low concentration of dissolved gas when the contents of a cavity are incapable of absorbing any significant amount of the work. Thus, almost all of the energy of collapse will be used to compress the surrounding liquid. The contents of a collapsing cavity have a significant retarding effect on the cavity collapse and the damage that results from it only when the vapor pressure is high compared to ambient pressure or when the dissolved-gas content is high. This behavior is called the thermodynamic effect (Ref 1, 2).

Erosion

The high-velocity impact of a drop of liquid against a solid surface produces two effects that result in damage to the surface: high pressure, which is generated in the area of the impact, and liquid flow along the surface at high speed radially from the area of impact, which occurs as the initial pressure pulse subsides. A first approximation of the average impact pressure, before radial outflow, is the idealized water-hammer pressure that would be generated from the impact between a flat-fronted liquid body and a flat rigid surface. Its value is ρCV, where ρ is the liquid density, C is the acoustic velocity of the liquid, and V is the impact velocity. For example, for water impacting at 480 m/s (1570 ft/s), this pressure is about 1100 MPa (160 ksi)—considerably above the yield strength of many alloys. This value is somewhat reduced by the compressibility of the surface.

In the impact of a spherical drop against a flat surface, the liquid/solid interaction is considerably more complicated; not yet fully understood, it has been a subject of controversy. However, there is now ample analytical and experimental confirmation (Ref 2) that the maximum pressure is developed not at the central point of impact but in a ring around it, and that this maximum pressure is close to twice the idealized water-hammer pressure referred to above (Ref 3). More specifically, as the instantaneous contact area between the impacting drop and the surface increases, the pressure at the perimeter of this area also increases until finally relieved by gross radial outflow of liquid from the impact area. Microscopic observation of damage caused by single impacts has revealed an annular zone of deformation, and sometimes tearing or cracking, which has been attributed to outward-flowing liquid with high superimposed pressures. A central depression is also observed in very ductile metals.

In liquid impingement, each collision between a drop of liquid and a surface can

established that the collapse of only 1 in 30 000 cavitation bubbles results in visible surface damage (Ref 1).

One model for liquid-impingement erosion processes is illustrated in Fig. 3. The impact-pressure history (and resulting stress waves) can produce circumferential cracks or deformation patterns around the initial area of impact (Fig. 3a), depending on the properties of the surface material and the energy of the impact. Following impact, the liquid flows away radially at high velocity. The spreading liquid may hit nearby surface asperities or the surface steps resulting from plastic deformation caused by the initial impact pressure. The force of this impact stresses the asperity or surface step at its base and may produce a crack (Fig. 3b). Subsequent impacts by other drops may widen the crack or detach a particle entirely (Fig. 3c). Direct hits on existing cracks, pits, or other deep depressions can produce accelerated damage by a microjet-impingement mechanism (Fig. 3d). Eventually, the pits and secondary cracks intersect, and larger pieces of the surface become detached.

Characteristics of Erosion Damage

Materials may be damaged by deformation, ductile fracture, brittle fracture, or fatigue. Corrosion was once thought to play an essential role in cavitation erosion, but some experiments (most notably, tests of plastics in water and of aluminum in toluene) strongly indicate that damage can occur even with the complete lack of corrosion. This does not mean that corrosion does not influence damage in situations where corrosion is known to occur, but rather that corrosion is not a necessary factor in producing damage. However, it may increase total damage considerably (up to tenfold) compared to the mechanical components alone (Ref 2).

Fig. 3 Processes by which a material is damaged by liquid-impingement erosion

(a) Solid surface showing initial impact of a drop of liquid that produces circumferential cracks in the area of impact or produces shallow craters in very ductile materials. (b) High-velocity radial flow of liquid away from the impact area is arrested by a nearby surface asperity, which cracks at its base. (c) Subsequent impact by another drop of liquid breaks the asperity. (d) Direct hit on a deep pit results in accelerated damage, because shock waves bouncing off the sides of the pit cause the formation of a high-energy microjet within the pit.

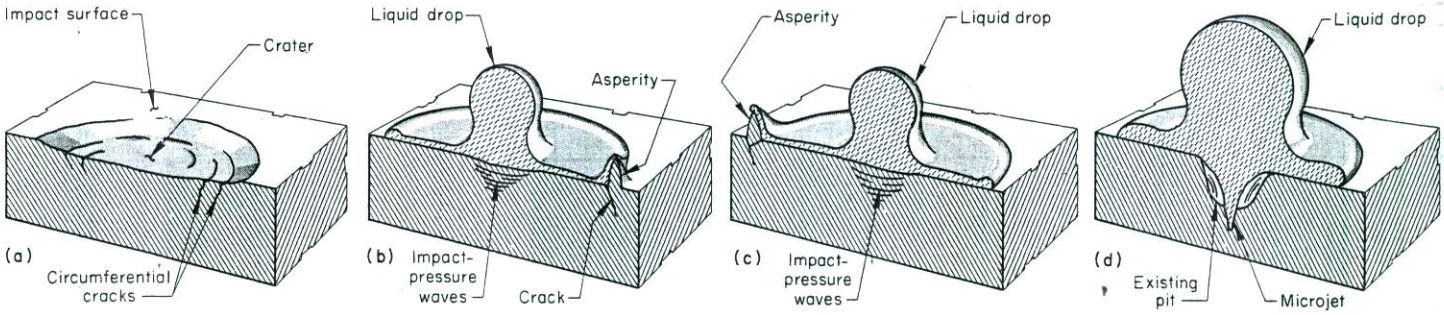

In ductile materials, liquid erosion often occurs by the formation of microscopic craters under the impact of cavitation shock waves, drop impingement, or microjet impingement, as shown in Fig. 4(a) for polycrystalline nickel exposed to intense cavitation in a standard vibratory cavitation test for 5 s at 20 kHz. Longer exposure times result in more widespread damage and a deepening of previously formed shallow pits (Fig. 4b) and eventually in fracture of extruded ridges between adjacent pits (Fig. 4c). Metallographic examination and x-ray diffraction studies have shown that plastic deformation—in the form of both slip and mechanical twinning—can occur in a layer about 30 to 300 μm below the surface during the initial stages of damage. This layer remains fairly constant in thickness throughout the subsequent stages of material removal. Apparently, material is lost by ductile fracture of asperities in the early stages of the erosion process, with fracture of work-hardened surface material and of ridges between erosion pits predominating in later stages. Brittle materials are eroded mainly by fracture and chipping of microscopic particles from the surface.

Experimental evidence has convincingly shown that some erosion damage is the result of single events. Pits observed on erosion-test specimens after short exposures are often essentially unchanged after much longer exposures (Ref 1, 2). However, because fatigue striations are occasionally found on a damaged surface, fatigue cannot be dismissed as a possible damage mechanism. Figure 5 illustrates damage on a stainless steel pump component; erosion occurred in cavitating mercury (Ref 1, 2). Large individual craters are scattered over a background of typical small-scale pitting. Regions of fatigue also were found on this component.

Erosion Rates. The rate of cavitation or liquid-impingement erosion, commonly measured as weight or volume loss per unit of time, often follows one of the patterns shown in Fig. 6. Erosion damage of most materials is not observable as a weight loss until after an incubation period. The erosion rate then usually rises rapidly to a maximum, which may persist for some time, as shown by the dashed curve in Fig. 6, then it usually decreases to a lower value, which either may remain relatively steady or may fluctuate unpredictably. The length of the incubation period, the maximum damage rate, and the shape of subsequent portions of the erosion-rate curve depend on the intensity of cavitation or liquid impingement, the properties of the material, and (to a minor extent) the original surface condition. A smoother surface often increases the incubation period, but does not affect maximum damage rate. At low hydrodynamic intensities, the chemical activities of the material and the environ-

Fig. 4 Scanning electron micrographs of a surface of polycrystalline nickel damaged by exposure to intense cavitation in a vibratory test at 20 kHz

(a) Shallow craters that formed on the surface after exposure for 5 s. (b) More widespread and deeper attack after exposure for 10 min. (c) Fracture of ridges between deep pits after exposure for 2 h. Source: Ref 4

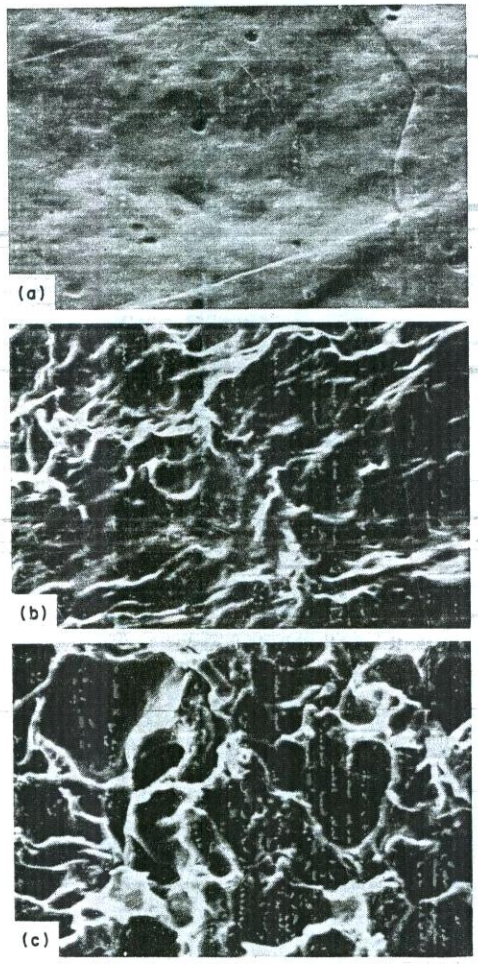

Fig. 5 Pitted surface of a stainless steel pump component damaged by exposure to cavitating mercury

Source: Ref 1, 2

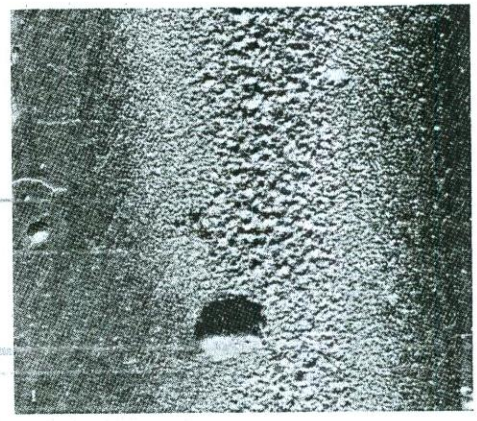

Fig. 6 Schematic representation of typical variation of liquid-erosion rate with exposure time

See text for discussion.

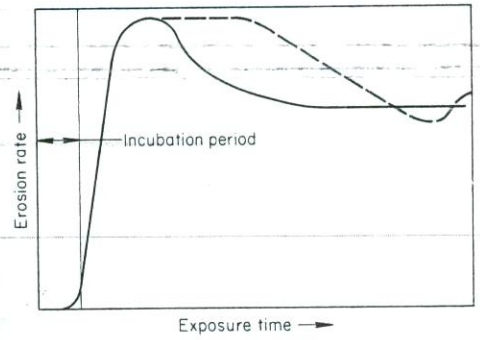

work-hardened layer mentioned previously. During this time, only random surface pitting occurs with a very slight loss of microscopic particles from widely separated locations on the surface. As detectable weight loss begins, the characteristics of the surface change, with fracture, deep pitting, and fatigue becoming more evident. The exact mechanisms vary with the properties of the material and with the hydrodynamic intensity. Reduction of the damage rate appears to occur when the surface has become so rough that the intensity of individual impacts is reduced by the presence of liquid

tions in the erosion rate may occur because of gross changes in part contour.

Effect of Flow Velocity. There have been several attempts to correlate the rate of erosion with flow properties of the fluid stream (for cavitation) and with impact velocity of drops (for liquid impingement). Although the results have not been adequately explained by any theory proposed to date, the maximum rate of volume loss per unit of area (sometimes expressed as the mean depth of penetration rate, MDPR) usually varies approximately with an exponential function of the relative velocity between surface and fluid.

In cavitation erosion, the exponent six is most commonly found, but exponents as high as ten and as low as two have been found for the dependence of MDPR on relative velocity (Ref 1, 2). The value of the exponent in a given instance is undoubtedly affected by such factors

In liquid-impingement erosion, the rate of volume loss usually varies with the fifth or sixth power of relative velocity. However, exponents as high as eight to ten have been determined for rain-erosion tests of some nonmetallic materials. Regardless of whether damage occurs by cavitation erosion or liquid impingement, the life of a component in a given erosive situation can be profoundly affected by small changes in relative velocity between the component and the eroding fluid.

Effect of Droplet or Jet Size. Erosion is also dependent on the size of impacting droplets or jets. For a given total mass of liquid impinging, the erosion will be less with smaller drops, even though this results in a larger number of impacts. However, a complete functional dependence and physical explanation is still lacking.

Damage Resistance of Metals

The resistance of specific metals or other materials to liquid erosion, which is commonly evaluated by ASTM G 32 (Ref 5), does not depend on any one property, although many attempts have been made to correlate erosion damage with different intrinsic properties. Various properties, such as hardness, ultimate resilience (one-half the square of ultimate strength divided by the modulus of elasticity), true stress at fracture, strain energy to fracture, corrosion-fatigue strength, and work-hardening rate, appear to be measures of resistance to erosion damage for certain metals or limited classes of alloys; ultimate resilience and hardness appear to be best (Ref 1, 2). However, most such correlations break down when attempts are made to extend them to a wide variety of alloys or to metallic and nonmetallic materials (Ref 6). Even elaborate correlations are often in error by as much as 300%, and for untested materials, they may predict erosion rates that are in error by an order of magnitude or more from the actual rate determined by subsequent testing. Brinell or Vickers hardness appears to be as good a correlating factor as any; its utility is enhanced by its widespread use as a measure of material strength. For many alloys, MDPR varies inversely with HB^n, where the exponent n has a value of about 2. This corresponds to ultimate resilience (Ref 1), which is consistent with an energy-to-brittle fracture model.

Part of the uncertainty involved in developing meaningful correlations is due to the uncertain definition of exposure conditions that produce damage in various laboratory-test mechanisms. Even more influential is that different mechanisms of metal removal appear to exist, depending on the intensity of the cavitation or impingement and the relative importance of corrosion. Intense hydrodynamic conditions seem to favor single-event processes, but conditions that produce impacts of a lesser magnitude are more conducive to fatigue or to corrosion enhanced by the mechanical removal of protective films of corrosion products.

Effect of Hardness. Hardness is usually a good index of erosion resistance when the same alloy or very similar alloys are considered at different hardness levels. However, erosion resistance of different types of alloys at the same hardness level may vary by an order of magnitude or more.

In some instances, work hardening can increase erosion resistance, especially under mild erosive conditions. However, for long exposures or for intense exposure conditions, erosion resistance may be reduced, probably because work hardening by the eroding medium precedes loss of material by fatigue or fracture. Surface treatments such as shot peening are generally not very effective, because they duplicate the processes that occur during the incubation period.

Thermal treatments, especially those that increase toughness as well as hardness, usually improve erosion resistance. Generally, a ductile and work-hardenable metal of a given hardness will resist erosion better than a brittle metal of the same hardness.

Laboratory experiments and service experience universally confirm that the Stellites, a family of cobalt-chromium-tungsten alloys, are the most resistant of all the structural alloys to liquid erosion. Although the erosion resistance of Stellite alloys is approached by that of some high-strength ausformed or maraging steels and may be equaled by that of some very hard tool steels, the Stellites achieve outstanding erosion resistance with lower hardness and greater resistance to corrosion and stress-corrosion cracking than either high-strength steel or tool steel. Relative to their hardnesses, titanium alloys and the Inconel nickel-base alloys exhibit above average erosion resistance.

Effect of Microstructure. Small grain size and fine dispersions of hard second-phase particles enhance erosion resistance. These characteristics, particularly the latter, appear to give the Stellites and some tool steels their superior erosion resistance.

Some investigations have shown that cavitation impacts induce phase transformations in certain highly erosion-resistant materials, including Stellites and some work-hardening chromium-manganese steels. It has been proposed, but not proven, that the energy absorbed in the transformations contributes to their high erosion resistance.

Ranking for erosion resistance in a given situation is made difficult by the complications of defining both the fluid conditions that result in damage and the metal properties that influence erosion resistance. This is true for laboratory tests and for field evaluations. Even as late as 1960, attempts to rank materials for cavitation resistance produced only a qualitative comparison, because results from different sources varied widely in cavitation conditions and in amount of damage for the same material.

A ranking system that is at least semiquantitative has been developed (Ref 6, 7). In this system, the value of a normalized erosion resistance, defined as the maximum rate of volume loss of a reference material divided by the maximum rate of volume loss for the material being evaluated, is computed. This allows comparison of materials that have been tested under different sets of conditions, provided that the reference material has been tested under each of the different sets of conditions. Figure 7 is a summary of normalized erosion resistance for a wide variety of alloys tested at different conditions, using 18Cr-8Ni austenitic stainless steel with a hardness of 170 HV as the reference material. Figure 7 shows that the most resistant alloys (tool steels, Stellite alloys, and maraging steels) have greater erosion resistance than the reference material, by an order of magnitude or more, and the range of normalized erosion resistance spans almost four orders of magnitude. This range is far greater than any range of intrinsic material properties. For these reasons, the present lack of precision in erosion prediction is not surprising.

Prediction of Erosion Rates. In cavitation, the hydrodynamic conditions are so difficult to describe that no quantitative erosion prediction equation, based on independently measurable parameters, exists. In liquid impingement, however, it is sometimes possible to predict erosion rates based on known values of the amount of liquid impinging, the impact angle and velocity, and perhaps the droplet size. Although theoretically based analytical models for erosion rates have been published, none has yet succeeded in predicting all the empirically observed relationships; some yield erosion rates that are in error by a factor of 10 000 or more.

At the current state of knowledge, better predictions can be made by purely empirical equations derived from compilations of test data. One such equation is given in Ref 6. A development of the same approach, using data from an interlaboratory test program sponsored by ASTM Committee G-2, is given in Ref 7 and summarized below. Equation 1 predicts the maximum erosion rate (the peak in Fig. 6) and cannot be used for long-term extrapolations; it applies to impingement by water droplets or jets:

$$\log R_e = 4.8 \log V_0 + 0.67 \log d + 0.57J - 0.22K - 16.65 - \log \text{NER} \qquad \text{(Eq 1)}$$

where R_e is the rationalized erosion rate, or volume of material removed per unit volume of water impinged, on same area; V_0 is the normal (to surface) component of impact velocity in meters per second; d is the typical droplet or jet diameter in millimeters; J is 0 for impact by droplets, or 1 for lateral impact by cylindrical jets; K is 0 for flat target surfaces, or 1 for curved or cylindrical target surfaces; and NER is the erosion resistance number, essentially identical to the normalized erosion resistance

Fig. 7 Classification of 22 alloys or alloy groups according to their normalized erosion resistances relative to 18Cr-8Ni austenitic stainless steel having a hardness of 170 HV

Source: Ref 6

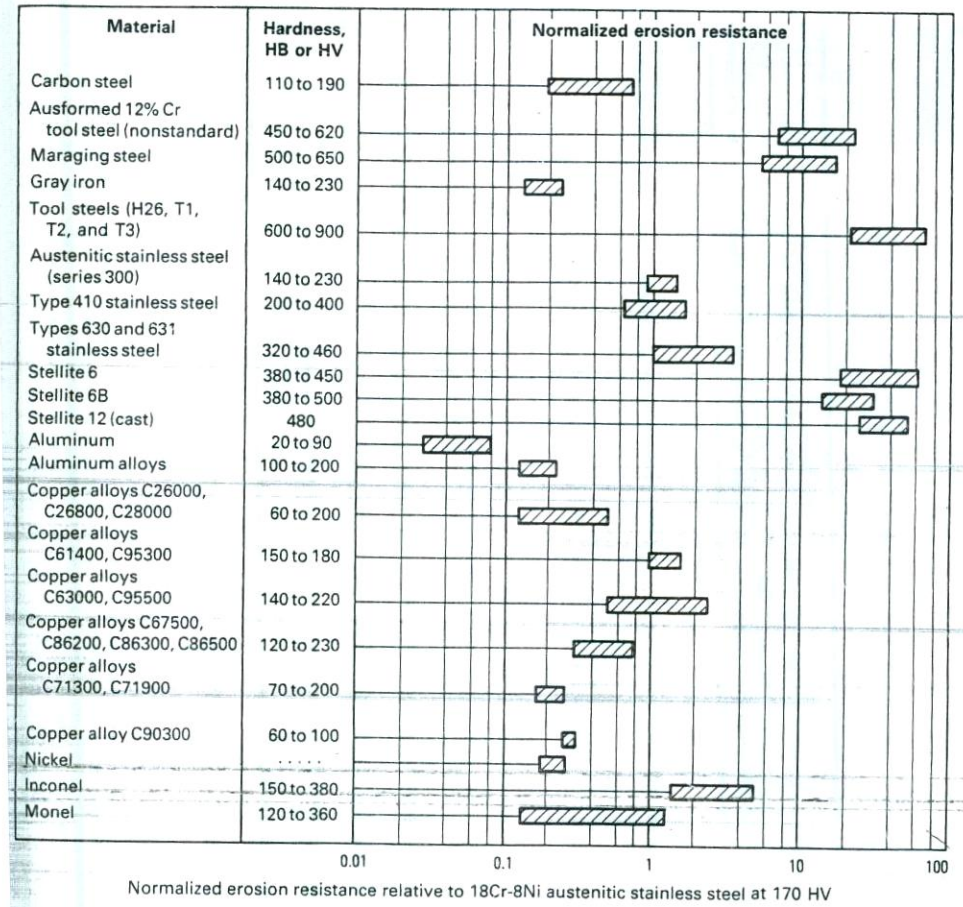

of Ref 6 and Fig. 7. There is some evidence that for liquids other than water, an additional factor of 2 log G, where G is the specific gravity of the liquid, should be added. The expected or mean prediction error for Eq 1 is about a factor of three; in some instances, the actual error will be an order of magnitude or more.

Effect of Corrosion

Liquid erosion is known to occur in the absence of any direct evidence of corrosion, yet corrosion can markedly influence the erosion process. Liquid erosion was once thought to be exclusively a corrosion-enhanced process. According to the corrosion theory, collapsing cavitation bubbles cause the mechanical removal of protective surface films. The newly exposed metal surface immediately begins to corrode, forming another film. Repeated removal and re-formation of the film of corrosion products produces the characteristic pitting attack. Although largely rejected as the basic mechanism of liquid erosion, the erosion-corrosion process described above can drastically accelerate erosive attack, particularly at low hydrodynamic intensities in aggressive environments. At very high hydrodynamic intensities, corrosion is rarely a significant factor, even in aggressive environments.

Because corrosion was once thought to be basic to liquid erosion, cathodic protection was investigated as a means of reducing erosive damage, revealing that cathodic protection did reduce damage. However, it now appears that damage was reduced only when the applied current density was sufficient to generate a layer of hydrogen bubbles on the tested surface. Thus, damage may have been reduced primarily because the layer of hydrogen bubbles cushioned the surface against the hydrodynamic forces of bubble collapse rather than because the cathodic current provided galvanic protection. Cathodic protection will of course reduce total weight loss when corrosion is a significant factor in producing damage. Nevertheless, recent experiments have shown that damage is also sometimes reduced when an anodic current of sufficient density to evolve gas at the tested surface is applied.

Fig. 8 Leading edge of a series 400 stainless steel impeller for a boiler feed pump showing deep local damage caused by cavitation erosion

Source: Ref 1, 2

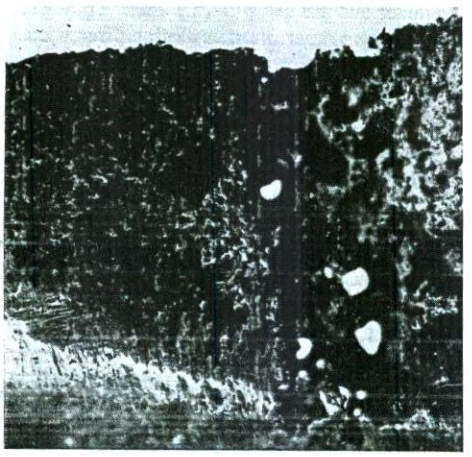

Analysis of Liquid-Erosion Failures

Erosion damage typically appears as a pitted or honeycomblike region, as shown in Fig. 8 on a stainless steel impeller blade from a boiler feed pump. In some instances, erosion damage results in an appreciable loss of metal. For example, the propellers of high-speed ocean liners have sustained sufficient loss of metal in a single crossing of the Atlantic to require replacement.

In hydraulic components, the damaged area will rarely be associated with the region of lowest static pressure. If low static pressure is the cause of cavitation, damage will be downstream of the low-pressure region where vapor pockets cannot be sustained and bubbles implode. It is a common misconception that cavitation damage can occur only in low-pressure regions. Cavitation damage often occurs in relatively high-pressure regions; this is particularly true if sufficiently high flow velocity also occurs. A complete determination of the local cavitation parameter for the flow, K_f, and an estimation of the probable value of the local parameter for incipient cavitation, K_i, can be valuable in establishing whether cavitation is responsible for observed damage (calculation of these parameters is discussed in Ref 1). Regardless of other environmental effects, the existence of drop impingement or hydraulic conditions conducive to cavitation should be positively ascertained before the damage is ascribed to liquid erosion.

Example 1: Failure of a Bronze Pump Impeller by Cavitation Damage. Figure 9(a) shows the impeller from one of two water pumps that were taken out of service because of greatly reduced output. Both impellers showed

considerable material loss over all the interior and exterior surfaces. The pumps drew water from an open tank through a standpipe. Several similar water pumps were operating under almost the same conditions with no observed failures.

The impellers were 25.4 cm (10 in.) in diameter and 1.3 cm (0.5 in.) wide. They were made from a cast bronze alloy and were contained in a cast iron pump casing.

Investigation. Visual examination of the impellers disclosed that the interior surfaces were extremely clean but were pockmarked over the entire area. The flange face on the suction side and the surfaces adjacent to those where material was missing showed evidence of cold work.

Micrographs of sections through the damaged surfaces showed a layer of distorted metal grains (Fig. 9b). At higher magnification, slip lines were visible, indicating that severe cold work had occurred at the surface. There was no evidence of intergranular attack or dezincification.

The clean, pockmarked, severely eroded surfaces of the impellers are characteristic of cavitation damage. In this instance, cavitation damage could have been the result either of a turbulent flow pattern caused by the movement of the impellers in the liquid or of excessive air in the system because the water in the supply tank was low or because air had been drawn through a pump seal. Further investigation revealed that considerable quantities of air were being drawn into the system when the water in the supply tank was allowed to drop to a low level.

Conclusions. Cavitation erosion caused the metal removal and the microstructural damage evidenced by a shallow layer of severely worked grains at the damaged surface. Cavitation was induced when a low level of water in the supply tank allowed large quantities of air to be drawn into the standpipe along with the water. However, air injection into the bubble-collapse region is sometimes used to reduce damage by cushioning bubble collapse (Ref 1, 2).

Corrective Measures. A water-level control was added to the piping system to maintain a sufficient head of water at the standpipe, and air was excluded from the pump inlet. No further failures occurred.

Example 2: Cavitation Erosion of a Water-Cooled Aluminum Alloy 6061-T6 Combustion Chamber. Equipment in which an assembly of in-line cylindrical components rotated in water at 1040 rpm displayed excessive vibration after less than 1 h of operation. The malfunction was traced to an aluminum alloy 6061-T6 combustion chamber (Fig. 10a) that was part of the rotating assembly.

The combustion chamber consisted of three hollow cylindrical sections having diameters of 7.5 cm (3 in.), 7.3 cm (2.875 in.), and 3.0 cm (1.1875 in.), respectively (left to right, Fig. 10a).

Investigation. Preliminary examination of the combustion chamber showed pitting on the water-cooled exterior surface in two bands approximately 0.64 cm (0.25 in.) wide that extended completely around the circumference of the chamber at axial locations of 4.8 cm (1.875 in.) and 9 cm (3.5625 in.) from the right-hand end of the 7.3-cm (2.875-in.) diam section of the chamber as shown in Fig. 10(a). The pitting was more severe in the band at the 4.8-cm (1.875-in.) location (particularly over about 180° of the circumference) than in the band at the 9-cm (3.5625-in.) location.

Also, a circumferential groove about 1.3 cm (0.5 in.) wide and having a maximum depth of about 0.25 mm (0.010 in.) had been abraded on the 7.5-cm (3-in.) diam section of the chamber along an arc of approximately 180° at the left edge in Fig. 10(a). At the point at which this wear was observed, the combustion chamber was designed to have a nominal clearance from a concentric housing around it, with cooling water flowing through the intervening annular space. The region of maximum wear was on the same side of the chamber as the region of severest pitting.

In operation, gases in the combustion chamber reached a very high temperature. The high thermal conductivity of the aluminum alloy, the rotation of the chamber, and axial flow of cooling water that was initially at room temperature provided efficient cooling of the chamber.

The 3.0-cm (1.1875-in.) outer-diameter shank served as the fuel inlet, and ignition took place within the main portion of the chamber. Accordingly, the shank was the coolest portion of the chamber and was not expected to be exposed to temperatures above about 95 °C (200 °F), even near the interior surface, on the basis of test data and calculations. Metal temperatures above about 175 °C (350 °F) were expected to be reached only to a very shallow depth on the interior surface in the hottest portions of the main body of the chamber, because of the high heat-transfer rate across the 8-mm (0.3125-in.) thick wall.

Spectrographic analysis showed that the material of the chamber corresponded in composition to aluminum alloy 6061, as specified. Tests also showed that the chamber had been anodized.

Hardness measurements taken at intervals all around the circumference of the chamber near the more severe band of pitting averaged 83 HB, with the lowest reading at 75 HB. The average hardness on the exterior of the shank was 83 HB. These hardnesses were substantially lower than the typical hardness of aluminum alloy 6061-T6, which is 95 HB.

Three cross-sectional specimens were taken for metallographic examination. Specimen 1 was taken through the most severely pitted area, and a portion of this specimen is shown at two magnifications in Fig. 10(b) and (c). This region was generally eroded to a depth of about 0.02 mm (0.001 in.), and some pits (not shown) were several thousandths of an inch

Fig. 9 Water-pump impeller with considerable loss of material from cavitation damage

(a) Photograph of cast bronze impeller. (b) Micrographs of an etched section from the impeller showing a layer of distorted metal grains at the surface subjected to cavitation. 100×

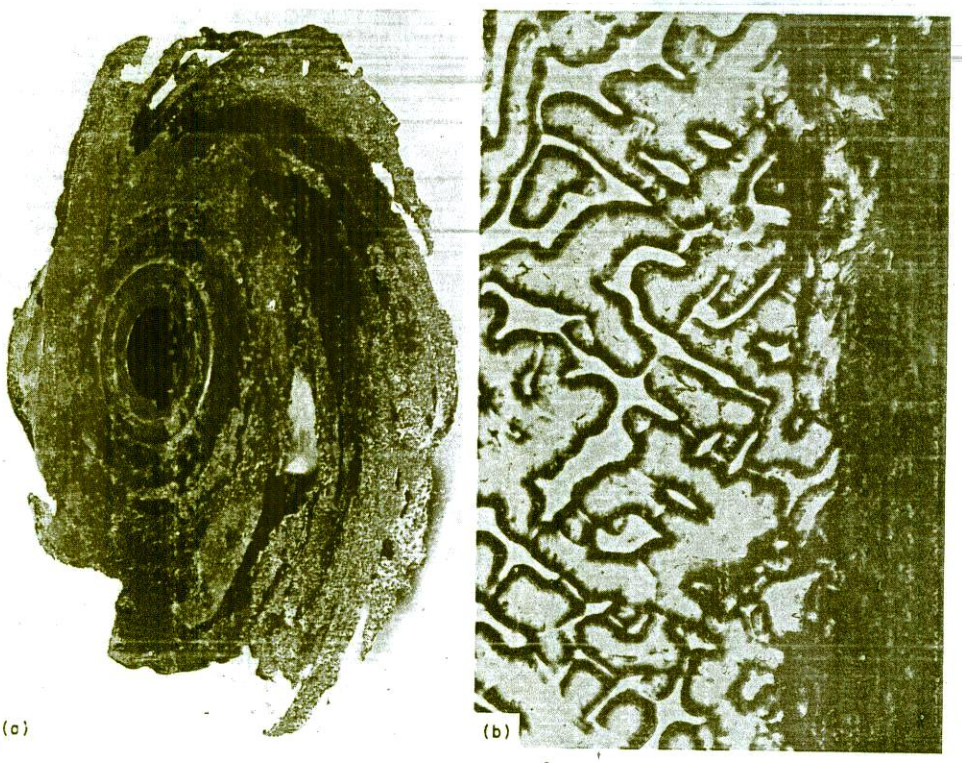

Fig. 10 Aluminum alloy 6061-T6 combustion chamber damaged by cavitation erosion

The chamber rotated in water at moderate speed. (a) Overall view of the chamber. (b) and (c) Micrographs of cross sections of the chamber wall showing typical cavitation damage. 100 and 500×, respectively

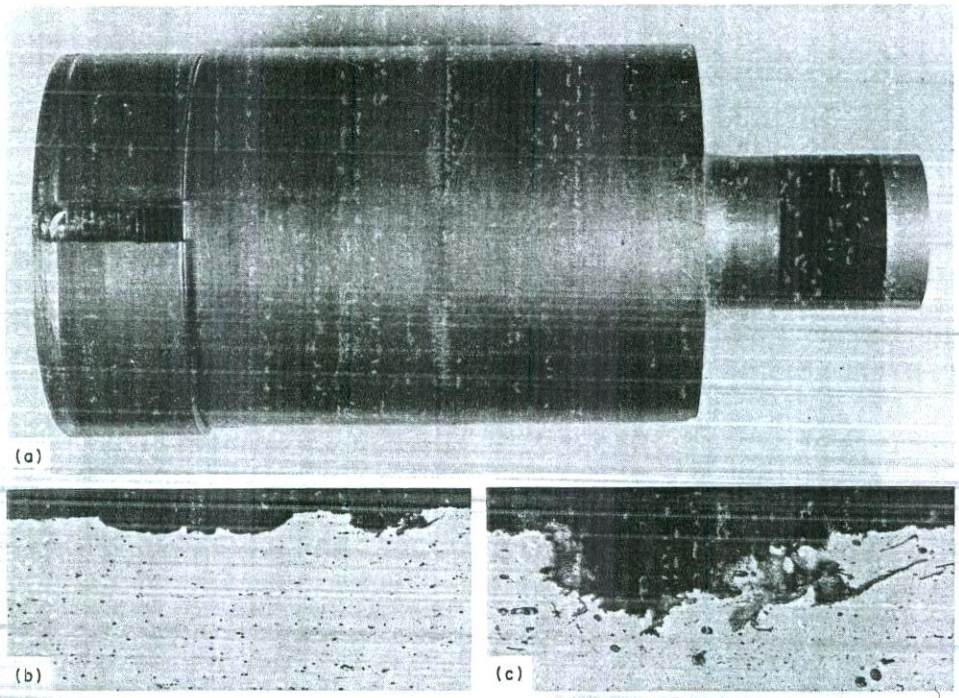

deep. This was also the area where the highest surface temperature on the chamber wall would be expected. Specimen 2 was taken through the most severely abraded region on the 7.6-cm (3-in.) outer diameter section of the part. Specimen 3 was taken through the shank, which was not damaged.

Examination of the three metallographic specimens at a magnification of 800× showed the structure to be essentially the same on each specimen and to contain a fairly dense distribution of a very fine precipitate of magnesium silicide (Mg_2Si) throughout the material. This constituent would be visible only if aluminum alloy 6061 had been heated to temperatures above about 175 °C (350 °F) or if it had been improperly heat treated.

Conclusions. As a result of improper heat treatment, the combustion-chamber material was too soft for successful use in this application. Because even the external surface of the shank, which could not be heated above about 95 °C (200 °F) in use, was just as soft and showed the same distribution of Mg_2Si as the hottest portion of the combustion chamber, overheating in service was eliminated as a possible cause of the observed low hardness.

Misalignment of the combustion chamber and one or both of the mating parts, to which the softness of the chamber material could have been a contributory factor, resulted in eccentric rotation and the excessive vibration that caused malfunction of the assembly. Contact against a surrounding member then caused the extensive abrasion shown at the left edge of Fig. 10(a). The pitting (which showed maximum severity on the same side of the chamber on which there was mechanical abrasion) was produced by cavitation erosion resulting from the combined effects of low hardness of the metal, cyclic pressure variation associated with the eccentric rotation (which induced the low pressures necessary for cavitation bubbles to form in the first place), and metal-surface temperatures near the boiling point of water at the hottest regions of the combustion-chamber exterior.

The operating characteristics of the defective combustion chamber were not sufficiently understood to explain the mechanism by which the cavitation erosion was concentrated at the two bands observed. Irregularities in the housing around the combustion chamber and temperature variation relating to the combustion pattern in the chamber were considered to be possible contributing factors to localization of the cavitation erosion.

Recommendations. The adoption of inspection procedures to ensure that the specified properties of aluminum alloy 6061-T6 were obtained and that the combustion chamber and adjacent components were aligned within specified tolerances was recommended to prevent future occurrences of this type of failure on these assemblies. In a similar situation, consideration should also be given to raising the pressure in the coolant in order to suppress the formation of cavitation bubbles.

Example 3: Liquid Erosion of Hydraulic Dynamometer Stator Vanes. Figure 11 shows severely eroded stator vanes of a hydraulic dynamometer for a steam-turbine test facility. The stator was cast from a copper-manganese-aluminum alloy. This type of dynamometer acts somewhat like a stalled hydraulic coupling: Vanes in the rotor impart tangential momentum to the water recirculating in a spiral path in the toroidal working compartment, and this momentum is killed by the fixed stator vanes. This results in dissipation of mechanical energy, which is converted into heat. The heat is carried away by a continuous through-flow of water superimposed on the recirculating flow. The water enters the working compartment through some of the holes that are visible in the stator vanes and exits through a circumferential slot between the rotor and stator at the outer diameter. The other stator holes vent the center of the recirculating vortex to the atmosphere. The resisting torque developed depends on the fill ratio, the thickness of the recirculating water film. The rate of water through-flow must be sufficient to maintain the temperature rise of the water within acceptable limits.

This dynamometer, designed to absorb up to 51 MW (69 000 hp) at 3670 rpm, constituted an extrapolation of previous design practices and experience. It was subject to severe erosion of the stator (Fig. 11) after relatively short operating times and initially required replacement of the stator after each test program. Up to 60 cm^3 (3.7 $in.^3$) of material was lost from each vane. However, even such severe erosion reduced its power-absorption capacity only slightly.

Investigation. The damage was clearly erosion by liquids, but it could not be firmly established—nor was there agreement in speculation—whether it was caused by cavitation or by liquid impact. It could be argued that cavitation is induced in the recirculating flow by the rotor vanes (acting as obstructions) or by the discontinuity of the water-discharge slot. It could also be argued that the acceleration forced on the water in the rotor, which makes the flow hug one side of each rotor pocket, causes a rotating discontinuous pattern of streams to emerge from the rotor, which then produces discrete liquid impacts on the stator vanes. A dynamic pressure transducer, installed in the working compartment, did show strong peaks at rotor vane frequency. Injection of air bubbles did not result in a reduction of fluctuation pressures in the working compartments, although this is a recognized method of controlling cavitation. Minor changes in geometry had little effect on erosion.

Recommendations. The remedy for this machine was a material substitution. The original stator casting material was changed to an Mo-13Cr-4Ni stainless steel (ACI designation CA-6NM). The original casting material has a normalized erosion resistance, N_e, of about 1; the CA-6NM, an N_e of 2 to 2.5. Consideration was given to Stellite cladding, but the CA-6NM

Fig. 11 Vanes of a dynamometer stator damaged by liquid erosion

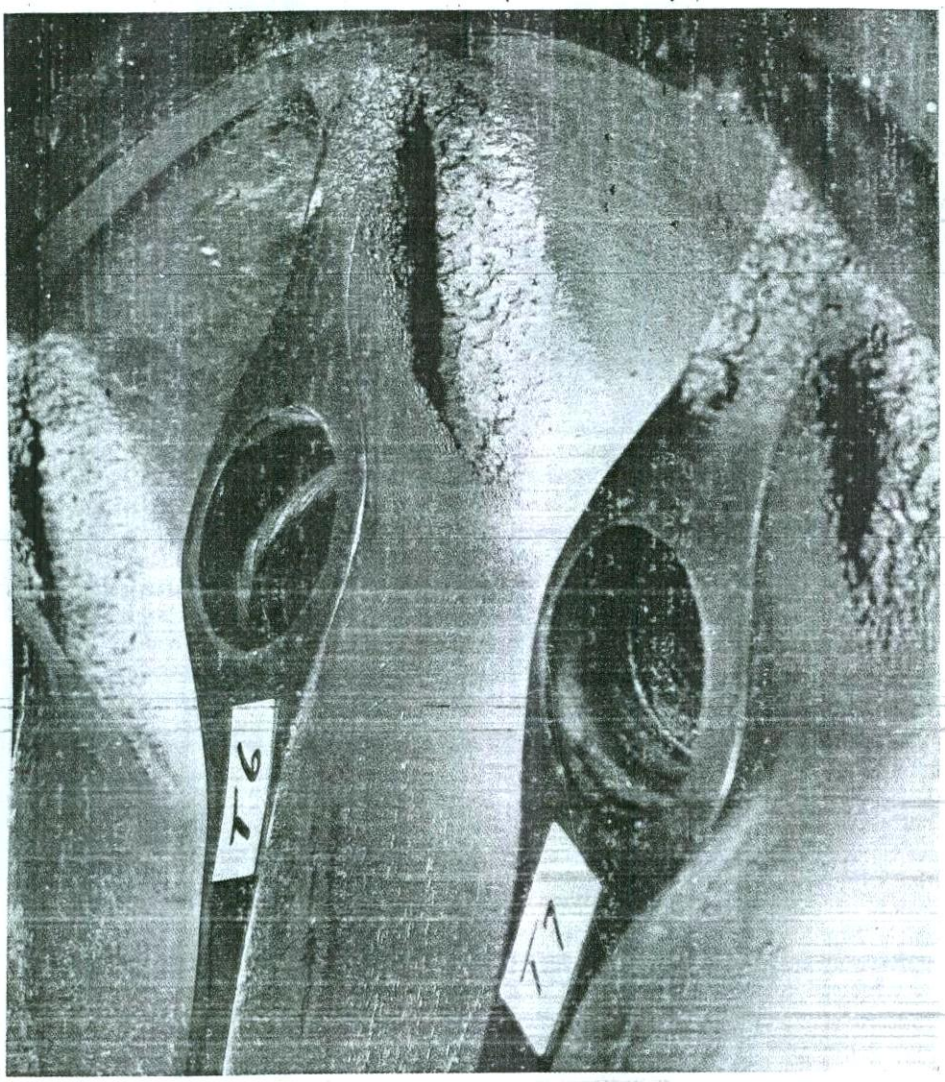

stators, while not erosion free, operated satisfactorily until the test facility was decommissioned. The dynamometer manufacturer has since radically redesigned its line of high-speed high-power dynamometers, with reduction of susceptibility to erosion (and to erosion-producing conditions) as one of the objectives.

Prevention of Erosion Damage

Damage from liquid erosion can be prevented or minimized by reducing the intensity of cavitation or liquid impingement, using erosion-resistant metals, or, under certain conditions, using elastomeric coatings.

Reduction of hydrodynamic intensity in devices subject to liquid impingement can be accomplished by reducing the quantity or size of liquid droplets in the gas stream, by reducing flow velocity, or both. In modern low-pressure steam turbines, for example, the problem of liquid erosion is attacked simultaneously by incorporating interstage moisture-removal devices, which reduce the amount of condensed water that can impinge on rotor blades in the following stage, by increasing the axial spacing between stator and rotor, resulting in smaller size and lower impact velocity of droplets, and by attaching shields of a Stellite alloy or hardened tool steel to the leading edges of rotor blades or locally flame hardening the leading edges, either of which provides the region subject to the greatest damage with a highly erosion-resistant surface layer. Stellite alloys have been used in the form of brazed-on strip, weld-deposited overlay, and laser cladding. Very hard wear-resistant coatings such as tungsten carbide often have not been successful for erosion protection.

In devices subject to cavitation, it may be possible to reduce the hydrodynamic intensity simply by increasing the radius of curvature of the flow path or by removing surface discontinuities. Both of these factors can significantly reduce the probability of cavitation. Increasing the cross section of flow passages will reduce flow velocity, thus reducing the intensity of cavitation. Also, entrained gas in a cavitating liquid reduces collapse pressures by a cushioning effect; consequently, damage can sometimes be reduced by the injection of controlled amounts of air into the liquid. Air injection is often used to reduce damage to certain hydraulic structures, such as dam spillways (additional information on cavitation in hydraulic equipment is available in Ref 1).

Use of Erosion-Resistant Metals. It may be impossible to reduce the hydrodynamic intensity significantly without seriously degrading performance. In such instances, the use of erosion-resistant metals may be the only practical solution to a problem of liquid erosion.

Many of the erosion-resistant metals can be applied as welded overlays; this makes salvage or repair of damaged surfaces easier or surface treatment of new components less costly than would be possible if the component had to be made entirely of erosion-resistant metal. Because liquid erosion is basically a surface phenomenon, the use of erosion-resistant overlays is effective in combating damage. The Stellite alloys and stainless steels are the alloys most widely used as overlays.

For example, Fig. 12 shows two portions of the leading edge of a blade from the last stage of a low-pressure steam turbine. One portion (at left, Fig. 12) was protected by an erosion shield of Stellite 6B; the other portion (at right, Fig. 12) was unprotected type 403 (modified) stainless steel. The shield made of 1-mm (0.04-in.) thick rolled strip and brazed onto the leading edge, resisted erosion quite effectively, but the unprotected base metal did not.

Both blade portions shown in Fig. 12 also illustrate the dependence of erosion on hydrodynamic intensity. Damage was most severe at the leading edge, where hydrodynamic intensity was greatest. Away from the leading edge, impacting droplets were smaller, impact velocity was lower, and impact occurred at oblique rather than right angles; therefore, damage was progressively less severe. The normal velocity component is important in erosion.

Many small parts are not amenable to protection by the use of erosion-resistant overlays. Therefore, the most effective means of combatting erosion of small parts is to increase the hardness of the metal or to specify a more erosion-resistant metal.

Use of Elastomeric Coatings. Some devices, particularly those that operate in regions of low hydrodynamic intensity, have successfully resisted erosion when covered with a layer of a flexible material. Highly flexible materials, such as elastomers, are particularly resistant to cavitation erosion (and sometimes impact erosion), especially for low hydrodynamic intensities. In fact, under certain conditions, the erosion resistance of elastomers exceeds that of metal having considerably greater mechanical properties. For example, polyurethane coatings

Fig. 12 Two portions of a modified type 403 stainless steel steam-turbine blade damaged by liquid-impingement erosion

The portion at left was protected by a shield of 1-mm (0.04-in.) thick rolled Stellite 6B brazed onto the leading edge of the blade; the portion at right was unprotected. Compare amounts of metal lost from protected and unprotected portions. Both 2.5×

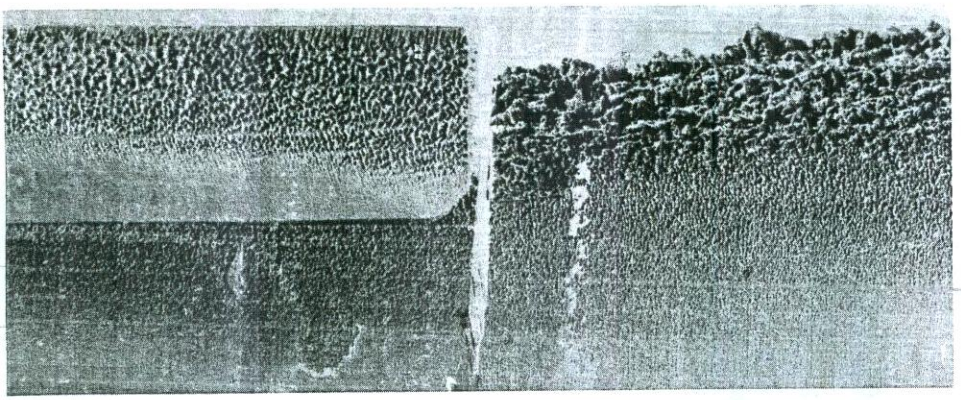

are widely used to protect radomes and some aluminum alloy surfaces of subsonic aircraft from rain erosion.

The resistance of elastomers to cavitation damage can be partly explained by the observed behavior of microjets during cavitation-bubble collapse near an elastomeric surface. In contrast to the tendency of microjets to be attracted toward rigid surfaces, microjets tend to be repelled from elastomeric or other highly flexible surfaces and dissipate their energy into the fluid rather than against the surface, due to effects on bubble-collapse dynamics near a flexible surface (Ref 1, 2). Theoretical analysis using a simple ideal fluid has verified that a flexible surface acts like a free surface, repelling collapsing bubbles, which are then attracted to any nearby rigid surface.

Elastomers can absorb energy by viscoelastic deformation. This allows them to resist liquid impacts at low hydrodynamic intensities. Impact stresses are attenuated because of the low acoustic impedance of the elastomer compared to that of metals, and the energy of individual impacts is dissipated within the elastomer. However, at high hydrodynamic intensities, the heat generated by the dissipation processes is excessive and causes decomposition and other forms of thermal failure characteristic of these materials.

Flexible coatings, especially rubber, have significant disadvantages; they are difficult to bond to some metals and to complex shapes and are susceptible to damage when short periods of high hydrodynamic intensity are encountered in an otherwise low-intensity environment. Intense cavitation sometimes destroys the bond between a relatively thin layer of rubber and the substrate, perhaps due to temperature buildup in the bond due to cold work.

REFERENCES

1. R.T. Knapp, J.W. Daily, and F.G. Hammitt, *Cavitation*, McGraw-Hill, 1970
2. F.G. Hammitt, *Cavitation an d Multiphase Flow Phenomena*, McGraw-Hill, 1980
3. F.J. Heymann, High-Speed Impact Between a Liquid Drop and a Solid Surface, *J. Appl. Phys.*, Vol 40, 1969, p 5113-5122
4. B. Vyas and C.M. Preece, Residual Stresses Produced in Nickel by Cavitation, in *Proceedings of the 4th International Conference on Rain Erosion and Allied Phenomena*, A.A. Fyall, Ed., Royal Aircraft Establishment, London, 1975
5. "Standard Method of Vibratory Cavitation Erosion Test," G 32, *Annual Book of ASTM Standards*, Vol 03.02, ASTM, Philadelphia
6. F.J. Heymann, *Toward Quantitative Prediction of Liquid Impact Erosion*, STP 474, ASTM, Philadelphia, 1970, p 212-248
7. "Standard Practice for Liquid Impingement Erosion Testing," G 73, *Annual Book of ASTM Standards*, Vol 03.02, ASTM, Philadelphia

SELECTED REFERENCES

- A Discussion on Deformation of Solids by the Impact of Liquids, *Philos. Trans. R. Soc. (London) A*, Part No. 1110, 1966
- *Characterization and Determination of Erosion Resistance*, STP 474, ASTM, Philadelphia, 1970
- P. Eisenberg, H.S. Preiser, and A.T. Thiruvengadam, How to Protect Materials Against Cavitation Damage, *Mater. Des. Eng.*, March 1967
- *Erosion by Cavitation or Impingement*, STP 408, ASTM, Philadelphia, 1967
- *Erosion, Wear, and Interfaces with Corrosion*, STP 567, ASTM, Philadelphia, 1974
- F.G. Hammitt, Cavitation, in *Handbook of Fluids and Fluid Machinery*, John Wiley & Sons, 1986
- F.G. Hammitt, Cavitation and Liquid Impact Erosion, in *Wear Control Handbook*, M.B. Peterson and W.O. Winer, Ed., American Society of Mechanical Engineers, New York, 1980, p 161-230
- C.M. Preece, Ed., *Treatise on Materials Science and Technology*, Vol 16, *Erosion*, Academic Press, 1979
- J.M. Robertson and G.F. Wislicenus, Ed., *Cavitation State of Knowledge*, American Society of Mechanical Engineers, New York, 1969
- T.R. Shives and W.A. Willard, Ed., *The Role of Cavitation in Mechanical Failures*, NBS 394, National Bureau of Standards, Washington, 1974
- *Symposium on Erosion and Cavitation*, STP 307, ASTM, Philadelphia, 1962